Available online at www.sciencedirect.com
ScienceDirect
Mechanical Systems and Signal Processing 21 (2007) 1041–1050
Mechanical Systems and Signal Processing
www.elsevier.com/locate/jnlabr/ymssp

Identification of bolted lap joints parameters in assembled structures

Hamid Ahmadian*, Hassan Jalali

Iran University of Science and Technology, School of Mechanical Engineering, Narmak, Tehran 16844, Iran

Received 30 April 2005; received in revised form 30 July 2005; accepted 11 August 2005
Available online 30 September 2005

Abstract

Bolted lap joints have significant influence on the dynamical behaviour of the assembled structures due to creation of strong local flexibility and damping. In modelling the dynamical behaviour of assembled structures the joint interface model must be represented accurately. A nonlinear model for bolted lap joints and interfaces is proposed capable of representing the dominant physics involved in the joint such as micro/macro-slip. The joint interface is modelled using a combination of linear and nonlinear springs and a damper to simulate the damping effects of the joint. An estimate of the response of the structure with a nonlinear model for the bolted joint under external excitations is obtained using the method of multiple scales. The parameters of the model, i.e. the spring constants and the damper coefficient, are functions of normal and tangential stresses at the joint interface and are identified by minimizing the difference between the model predictions and the experimentally measured data.

Keywords: Bolted lap joint; Nonlinear joint interface; Method of multiple scales

1. Introduction

All structural assemblies have to be joined in some way, by bolting, welding and riveting or by more complicated fastenings such as smart joints. It is known that the added flexibility introduced by the joint to the structure heavily affects its behaviour and when subjected to dynamic loading, most of the energy is lost in the joints. Determining the relevant physics of each joint is critical to a validated full body model of the structure. The two most common mechanisms of joint mechanics are frictional slip, and slapping [1]. These mechanisms have their own characteristic features, e.g. frictional slip becomes saturated at very high amplitudes and slapping pushes energy from low to high frequencies.

There are two common approaches used in identification of the joint properties. The first approach employs non-parametric identification methods and is widely used since no assumption about the properties of the joint is required. In this approach the joint flexibility and damping effects are modelled using added terms such as an equivalent excitation force which produces the same effects as a joint in the dynamic behaviour of the

*Corresponding author. Tel.: +98 21 73912907; fax: +98 21 77454050.
E-mail address: ahmadian@iust.ac.ir (H. Ahmadian).

0888-3270/$ - see front matter © 2005 Elsevier Ltd. All rights reserved.
doi:10.1016/j.ymssp.2005.08.015

structure. Crawley and Aubert [2] identified the properties of a structural joint using an experimental technique called "force-state mapping". In this method the force transmitted through a structural element such as a joint is regarded as the mechanical state of that element. Ren et al. [3] proposed a general purpose technique capable of identifying the force–response relationship of a nonlinear joint by treating the effects of the joint in the structure as an external force. They predicted the response using the principle of Multi-Harmonic Balance (MHB) and identified the dynamic characteristics of nonlinear joints using the experimentally measured responses. Ren and Beards [4] extracted joint parameters using measured frequency response functions of the structure. They used the difference between the dynamic properties of the sub-structures and the assembled structure and ideally supposed that this difference is caused by the joint effects. Ma et al. [5] studied the effects of a lap joint placed between two cantilever beams while the assembly is excited using a concentrated force acting parallel to the bolt axis. This type of excitation creates slapping at the joint interface in low bolt preload and high level of excitation. They treated the joint effects as an external force and identified the state of the joint by comparing the dynamic response of the bolted structure with the corresponding monolithic structure (the same structure without the joint). They experimentally obtained responses of the structure and observed non-proportional damping and nonlinear softening effects in the structure due to micro-impact in the bolted joint.

The second approach in modelling joints employs parametric models. In contrast with non-parametric models, in using the parametric models it is necessary to have a good understanding about the involved physics of a joint. Common phenomena in the joint interface are micro/macro-slips/slaps that cause energy dissipation and nonlinearity in the joints. Most parametric models are proposed to represent the nonlinearity and energy dissipation due to slip in the joints. Reviews on joint friction models are presented by Ferri [6], Gaul and Nitsche [7] and Ibrahim and Pettit [8]. A widely used model to represent the stick-slip response of the jointed structures is proposed by Iwan [9] consisting of a spring and a slider in series. Iwan used a combination of parallel/series spring-slider elements to describe the hysteresis behaviour of materials and structures. Song et al. [10] presented the so-called adjusted Iwan beam element to model the nonlinear effects of a bolted joint in assembled structures. Gaul and Lenz [11] used experimental observations and demonstrated that the behaviour of a lap joint in a rod like structure can be represented by an adjusted Iwan model. Their studies show that hysteresis loops measured at different excitation force levels have different slopes, i.e. as the level of force increases, the slope of hysteresis loop decreases, indicating a softening nonlinearity effect in the system. Hartwigsen et al. [12] used experimental observations to quantify the nonlinear effects of a typical shear lap joint in a beam with a bolted joint in its center, and in a frame with a bolted joint in one of its members. The experimental results showed several effects in the dynamics of structure attributed to the shear lap joint, namely reduction in the natural frequencies due to softening stiffness, nonlinear hardening damping effects, and slight distortions of the mode shapes, which alter drastically the measured FRFs. They also examined the ability of Iwan model to capturing the experimentally observed joint effects. Ouyang et al. [13] conducted experimental study on dynamic behavior of a single lap bolted joint experiencing slippage under different levels of bolt preload and excitations. They demonstrated as micro-slip develops in the joint, the hysteresis loop further deviates from an ellipse and there is more contribution from super-harmonics in the frequency spectrum. Existence of odd number super-harmonics in the frequency spectra indicates the existence of a cubic stiffness term in modelling. They also demonstrated that the Jenkins-element model can represent the joint friction in the sense that it is capable of reproducing the experimentally measured hysteresis loops.

In the current work a parametric model for the bolted lap joints is presented. The proposed model consists of a combination of linear and nonlinear springs with a viscous damper capable of representing the dissipation energy of the joint. A closed form solution for the frequency response of the assembled beam with nonlinear joint interface properties is obtained using the method of multiple scales. The calculated frequency response functions of the assembly with joint nonlinearity are then compared with the experimental observations to identify the joint parameters. In the experimental work the excitations force is applied parallel to the bolt axis and the force is kept at moderate level to create slip in the joint. In vicinity of the first mode of the beam assembly at moderate level of excitations, slipping is the dominant nonlinear mechanism at the joint interface. At higher level of excitations slapping may become the dominant effect. The parameters of the joint interface are identified by minimizing the discrepancies between the measured and the calculated frequency response functions.

2. Statement of the problem

The bolted structure considered in this work is shown in Fig. 1. It includes two identical linear Euler/Bernoulli free-free beams connected at one of their free ends by a bolted joint. A block mass is placed at one end of beam assembly in order to excite the joint interface adequately in the lower modes. Depending on the amount of bolt preload, one expects to observe nonlinear dynamical effects due to (a) dry friction at the area of contact of the beams leading to hysteresis loops in the force–displacement plots, and (b) micro-impacts or micro-slips caused by the looseness of the joint which leads to softening phenomena. Such nonlinear effects can drastically affect the dynamics of the bolted structure, and the proposed characterization methodology must be capable of modelling them accurately. The basic idea in the proposed methodology is to model the bolted joint interface with a nonlinear spring which resembles the softening effect of the joint interface at certain level of stresses in the interface.

The Euler–Bernoulli beam assembly considered here has a nonlinear flexibility at $x = L/2$ (see Fig. 1). The equations of motion for each part of the beam are:

$$EI\frac{\partial^4 W_1(x,t)}{\partial^4 x} + m\frac{\partial^2 W_1(x,t)}{\partial^2 t} = F(t)\delta(x), \tag{1}$$

$$EI\frac{\partial^4 W_2(x,t)}{\partial^4 x} + m\frac{\partial^2 W_2(x,t)}{\partial^2 t} = 0, \tag{2}$$

where EI, m, $W_1(x,t)$, $W_2(x,t)$ and $F(t)$ are flexural rigidity, linear mass density, lateral displacement at each of the two parts of the beam, and the point excitation on the beam at $x = 0$, respectively. The boundary conditions of the problem are defined as

$$\frac{\partial^2 W_1(0,t)}{\partial x^2} = \frac{\partial^3 W_1(0,t)}{\partial x^3} = 0, \quad EI\frac{\partial^3 W_2(L,t)}{\partial x^3} = M\frac{\partial^2 W_2(L,t)}{\partial t^2}, \quad EI\frac{\partial^2 W_2(L,t)}{\partial x^2} = -J\frac{\partial^3 W_2(L,t)}{\partial t^2 \partial x}, \tag{3}$$

where M and J are the mass and moment of inertia of the tip mass, respectively. Next we turn our attention to the compatibility requirements at the joint interface. To simplify the problem, one may neglect the mass effects of the joint interface and equate the bending moments and the shear forces of the two beam parts at the interface as

$$\frac{\partial^2 W_1(S,t)}{\partial x^2} = \frac{\partial^2 W_2(S,t)}{\partial x^2}, \quad \frac{\partial^3 W_1(S,t)}{\partial x^3} = \frac{\partial^3 W_2(S,t)}{\partial x^3}. \tag{4}$$

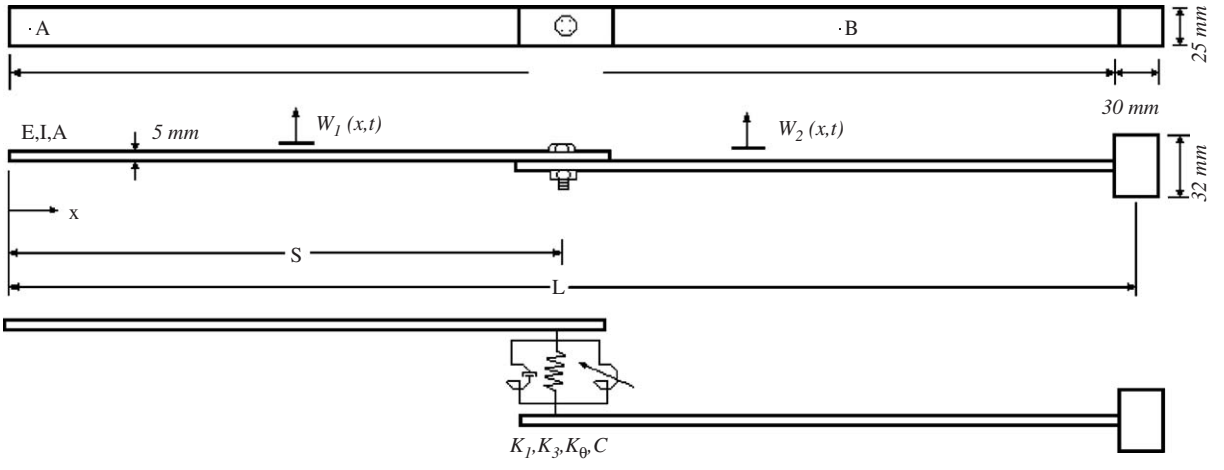

Fig. 1. The free–free beam/model with a lap joint.

Further compatibility requirements are defined by considering the joint interface behaviour. The shear stiffness of the joint is expressed using a linear translational spring, K_1, as

$$-EI\frac{\partial^3 W_1(S,t)}{\partial x^3} = K_1(W_2(S,t) - W_1(S,t)). \tag{5}$$

One may use a combination of linear and nonlinear springs to model micro-impact in the joint. In this paper the experiments are performed in vicinity of first resonant frequency. The excitation force produces micro-slips in the joint at these frequencies. This phenomenon can be modelled by considering a nonlinear bending stiffness for the joint. Therefore a combination of linear torsional spring, K_θ, a cubic torsional spring, K_3, and a torsional viscous damper, C is adopted to model the joint interface, i.e.

$$EI\frac{\partial^2 W_1(S,t)}{\partial x^2} = C\left(\frac{\partial^2 W_2(S,t)}{\partial t\partial x} - \frac{\partial^2 W_1(S,t)}{\partial t\partial x}\right) + K_\theta\left(\frac{\partial W_2(S,t)}{\partial x} - \frac{\partial W_1(S,t)}{\partial x}\right) - K_3\left(\frac{\partial W_2(S,t)}{\partial x} - \frac{\partial W_1(S,t)}{\partial x}\right)^3. \tag{6}$$

The cubic stiffness and viscous damping terms represent the saturation phenomenon and energy loss at the joint interface in the presence of high-level vibrations. In the following, solution to the above problem using the method of multiple scales is presented.

3. The analytical solution

In this section, solution of the governing equations stated in Eqs. (1) and (2), satisfying the compatibility requirements at the joint, along with the associated boundary conditions is sought. The method of multiple scales is applied directly to these equations. Solutions for each part of the beam are assumed of the forms:

$$W_1(x,t;\varepsilon) = W_{10}(x,T_0,T_1) + \varepsilon W_{11}(x,T_0,T_1), \tag{7}$$

$$W_2(x,t;\varepsilon) = W_{20}(x,T_0,T_1) + \varepsilon W_{21}(x,T_0,T_1), \tag{8}$$

where $T_0 = t$ is the fast time scale, and $T_1 = \varepsilon\, t$ is the slow time scale. Behaviour of the system is investigated near the resonance frequency. The linear undamped theory will predict unbounded oscillations at the resonance point no matter how small the excitation force is. In the considered system these large oscillations are limited by the damping and nonlinearity. Thus to obtain a uniformly valid approximate solution of this problem, one needs to order the excitation so that it will appear when the damping and the nonlinearity appear [14,15]. Therefore the forcing function, the nonlinear stiffness and the damping due to micro-slips are ordered as

$$\frac{F}{m} = \varepsilon f, \frac{C}{m} = \varepsilon\mu, \frac{K_3}{m} = \varepsilon K_N. \tag{9}$$

The derivatives with respect to the new time scales are defined as

$$\frac{\mathrm{d}}{\mathrm{d}t} = D_0 + \varepsilon D_1, \quad \frac{\mathrm{d}^2}{\mathrm{d}t^2} = D_0^2 + 2\varepsilon D_0 D_1, \quad D_n = \frac{\partial}{\partial T_n}. \tag{10}$$

Inserting the new variables into the system equations and sorting the obtained equations based on the orders of ε one obtains:

3.1. Order ε^0

The governing equations:

$$D_0^2 W_{10} + \frac{EI}{m} W_{10}^{iv} = 0, \quad D_0^2 W_{20} + \frac{EI}{m} W_{20}^{iv} = 0. \tag{11}$$

The boundary conditions:

$$W''_{10}(0,T_0,T_1)=W''_{10}(0,T_0,T_1)=0,$$
$$EI\,W'''_{20}(L,T_0,T_1)=MD_0^2W_{20}(L,T_0,T_1),$$
$$EI\,W''_{20}(L,T_0,T_1)=-JD_0^2W'_{20}(L,T_0,T_1). \tag{12}$$

The compatibility requirements:

$$W'''_{10}(S,T_0,T_1)=W'''_{20}(S,T_0,T_1),\ W^{'}_{10}(S,T_0,T_1)=W''_{20}(S,T_0,T_1),$$
$$EI\,W''_{10}(S,T_0,T_1)=K_\theta(W'_{20}(S,T_0,T_1)-W'_{10}(S,T_0,T_1)),$$
$$EI\,W'''_{10}(S,T_0,T_1)=-K_1(W_{20}(S,T_0,T_1)-W_{10}(S,T_0,T_1)). \tag{13}$$

3.2. Order ε^1

The governing equations:

$$D_0^2W_{11}+\frac{EI}{m}W^{iv}_{11}=f\cos(\Omega t)\delta(x)-2D_0D_1W_{10},$$
$$D_0^2W_{21}+\frac{EI}{m}W^{iv}_{21}=-2D_0D_1W_{20}. \tag{14}$$

The boundary conditions:

$$W'''_{11}(0,T_0,T_1)=W''_{11}(0,T_0,T_1)=0,$$
$$EI\,W'''_{21}(L,T_0,T_1)=MD_0^2W_{21}(L,T_0,T_1)+2MD_0D_1W_{20}(L,T_0,T_1),$$
$$EI\,W''_{21}(L,T_0,T_1)=-JD_0^2W'_{21}(L,T_0,T_1)-2JD_0D_1W'_{20}(L,T_0,T_1). \tag{15}$$

The compatibility requirements:

$$W''_{11}(S,T_0,T_1)=W''_{21}(S,T_0,T_1),$$
$$W'''_{11}(S,T_0,T_1)=W'''_{21}(S,T_0,T_1),$$
$$\frac{EI}{m}W''_{11}(S,T_0,T_1)=\mu D_0(W''_{20}(S,T_0,T_1)-W''_{10}(S,T_0,T_1))+\frac{K_\theta}{m}(W^{'}_{21}(S,T_0,T_1)-W^{'}_{11}(S,T_0,T_1))$$
$$-K_N(W^{'}_{20}(S,T_0,T_1)-W^{'}_{10}(S,T_0,T_1))^3,$$
$$EI\,W'''_{11}(S,T_0,T_1)=K_1(W_{11}(S,T_0,T_1)-W_{21}(S,T_0,T_1)), \tag{16}$$

where $(\,)'=\partial/\partial x$.

Assuming the response of the structure is dominated by a single mode, $Y_i(x)$, one may write the solution to the set of equations of order ε^0 as

$$W_{10}(x,T_0,T_1)=(A(T_1)e^{i\omega T_0}+cc)\,Y_1(x),$$
$$W_{20}(x,T_0,T_1)=(A(T_1)e^{i\omega T_0}+cc)\,Y_2(x), \tag{17}$$

where ω is the natural frequency of the structure and cc is the complex conjugate term for each part of the solution. The assumed solution transforms zero order equations to the following form:

$$Y_1^{iv}-\lambda^4Y_1=0,\quad Y_2^{iv}-\lambda^4Y_2=0,\quad \lambda^4=m\omega^2/EI \tag{18}$$

with the boundary conditions of the form:

$$Y'''_1(0)=Y'''_1(0)=0,\quad EI\,Y'''_2(L)=-M\omega^2Y_2(L),\quad EI\,Y'''_2(L)=J\omega^2Y'_2(L) \tag{19}$$

and the following compatibility conditions:

$$Y''_1(S)=Y''_2(S),\quad Y'''_1(S)=Y'''_2(S),\quad EI\,Y''_1(S)=K_\theta(Y^{'}_2(S)-Y'_1(S)),\quad EI\,Y'''_1(S)=-K_1(Y_2(S)-Y_1(S)). \tag{20}$$

The general solution of $Y_i, i = 1, 2$ are:

$$Y_1(x) = A_1 \sin(\lambda x) + B_1 \cos(\lambda x) + C_1 \sinh(\lambda x) + D_1 \cosh(\lambda x),$$
$$Y_2(x) = A_2 \sin(\lambda x) + B_2 \cos(\lambda x) + C_2 \sinh(\lambda x) + D_2 \cosh(\lambda x), \tag{21}$$

where the coefficients $A_i, B_i, C_i, D_i, i = 1, 2$, are obtained by satisfying the boundary conditions and the compatibility requirements.

The homogeneous Eqs. (11)–(13) have a non-trivial solution; therefore the non-homogeneous problem (14)–(16) will have a solution only if the solvability condition is satisfied. To determine this condition, the secular terms φ_i and non-secular terms V_i are separated by assuming a solution of the form:

$$W_{11} = \varphi_1(x, T_1)e^{i\omega T_0} + V_1(x, T_0, T_1) + cc,$$
$$W_{21} = \varphi_2(x, T_1)e^{i\omega T_0} + V_2(x, T_0, T_1) + cc. \tag{22}$$

The excitation frequency Ω is assumed to be close to the natural frequency of the dominant mode which governs the system response, i.e.:

$$\Omega = \omega + \varepsilon\sigma. \tag{23}$$

Substituting Eqs. (22) and (23) into the first-order Eqs. (18)–(20), secular terms are obtained as

$$\varphi_1^{iv} - \lambda^4\varphi_1 = -2i\omega Y_1 D_1 A + \frac{f}{2}\delta(x)e^{i\sigma T_1}, \tag{24a}$$

$$\varphi_2^{iv} - \lambda^4\varphi_2 = -2i\omega Y_2 D_1 A. \tag{24b}$$

Using the concept of the adjoint problem, one may obtain the solvability condition of the problem which ensures uniformity of the expansion of the dependent variables. To begin, Eq. (24a) is projected into its adjoint solution Y_1 over the range of $x = 0..S$, and Eq. (24b) is projected into its corresponding adjoint solution Y_2 over the range of$x = S..L$. Satisfying the boundary conditions along with the compatibility equations, one arrives at the following solvability condition:

$$3A^2\overline{A}K_N(Y_2'(S) - Y_1'(S))^4 - i\mu\omega A(Y_2'(S) - Y_1'(S))^2$$
$$- 2i\omega D_1 A\left(1 + \frac{M}{m}Y_2(L)^2 + \frac{J}{m}Y_2'(L)^2\right) + \frac{f}{2}Y_1(0)e^{i\sigma T1} = 0. \tag{25}$$

In extracting the solvability condition, one considers only the secular terms, i.e. the coefficient of $e^{i\omega T_0}$ and its conjugate, and neglects the coefficient of the other harmonies such as the third-order super-harmony $e^{i3\omega T_0}$and its conjugate $e^{-i3\omega T_0}$.

In a steady-state response the coefficient A is constant therefore Eq. (25) is simplified to the following frequency response equation:

$$\left[\left(\frac{\mu p}{2q}\right)^2 + \left(\sigma + \frac{3K_N a^2 p^2}{8\omega q}\right)^2\right]a^2 = \left(\frac{fY_1(0)}{2\omega q}\right)^2, \quad a = 2|A|, \quad p = (Y_2'(S) - Y_1'(S))^2, \quad q = 1 + \frac{M}{m}Y_2(L)^2 + \frac{J}{m}Y_2'(L)^2. \tag{26}$$

For identification purposes, one may compare the calculated frequency response function with the corresponding measured curve and fine tune the unknown parameters so that the analytical function and the measured values come to an acceptable agreement.

4. Experimental case study

Fig. 2 shows the test set-up for measuring the dynamic response of a bolted beam assembly. A tip mass is added to one end of the structure to increase the bending moment and transverse shear force at the joint interface. The suspended free–free structure is excited using a mini-shaker. The excitation force is applied in point A and the response of the assembled structure is measured at point B; both points are shown in Fig. 1. The bolt is tightened with a fixed preload which remains constant during the experiment.

Initially the structure is excited with a low-level pseudo-random force and the first three natural frequencies of the linear structure are obtained. Fig. 3 shows the corresponding FRF of the linear structure indicating three bending modes which are tabulated in Table 1. These modes will be used to identify the linear system defined in Eqs. (18)–(20).

Next the structure is excited using sinusoidal forces at two different force levels of 47.6 and 90.6 mN to obtain its linear and nonlinear responses. The linear and nonlinear frequency response functions of the beam measured at point B are shown in Fig. 4. The frequency response curves are obtained in the vicinity of the first mode by exciting the structure at each individual frequency and clearly demonstrate the joint softening

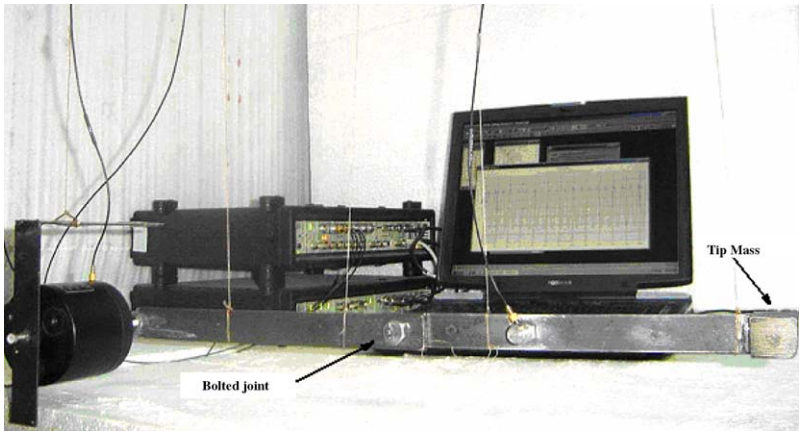

Fig. 2. The test set-up.

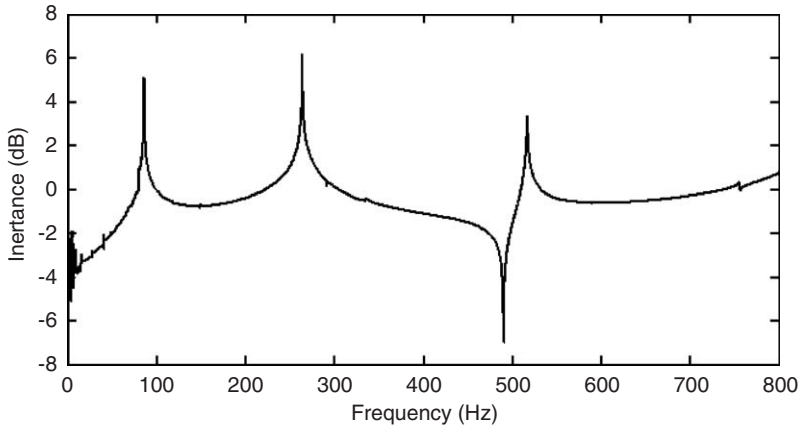

Fig. 3. The Frequency Response Function of the linear structure.

Table 1
Measured and predicted modes of the linear model

Mode no.	1	2	3
Measured (Hz)	86.44	264.37	517.37
Predicted (Hz)	86.44	265.63	518.28
Error (%)	0.0	0.48	0.18

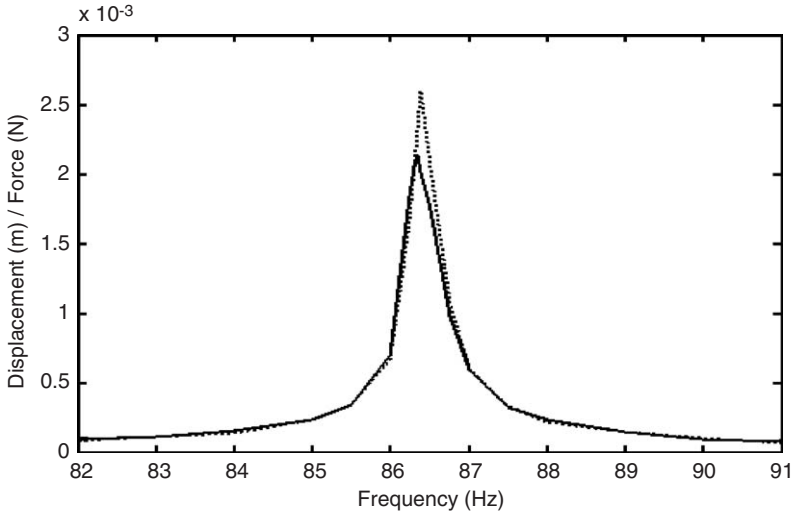

Fig. 4. The measured frequency responses at excitation levels 47.6 mN (dotted line), and 90.6 mN (solid line).

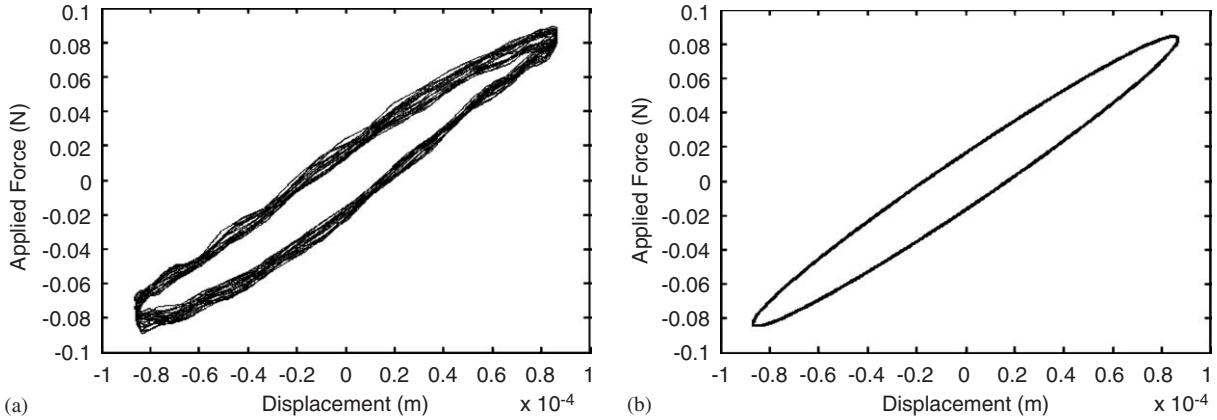

Fig. 5. The force displacement curve at 86.75 Hz, (a) the actual response, (b) the 3rd harmony is filtered from the response.

phenomenon due to micro-slips in the joint interface. The force at node A vs. the displacement at node B is shown in Fig. 5a. The curve clearly shows softening effect due to the joint properties. Analysing the response of the structure shows two common frequencies in the response, the excitation frequency and its third super-harmony, as expected. The third super-harmony produces softening effect in the force–displacement curve and when this harmony is omitted from the response as shown in Fig. (5b) the softening effect in the curve vanishes. In the next section the joint interface parameters are identified using the measured responses.

5. Identification of the joint parameters

The linear parameters of the joint, i.e. the lateral stiffness K_1 and the torsional stiffness K_θ, are identified using the first three natural frequencies of the linear system. This is achieved by minimizing the differences between the measured natural frequencies and the corresponding model predictions. Table 1 shows the results of updating of the linear model, indicating a good agreement between the two models.

The damping coefficient, C, and the nonlinear spring coefficient, K_3, are identified using the nonlinear response functions of the structure shown in Fig. 4. For a given excitation level, the peak amplitude of the

nonlinear frequency–response curve is a function of the damping value and K_3 produces the shift in the peak frequency. Thus, knowing the amplitude at the peak and the frequency shift, it is possible to estimate the damping coefficient and the effective nonlinearity of a system [16]. Differentiating Eq. (26) with respect to the detuning parameter σ and setting the results to zero to get the peak location, one finds the following relations between the peak amplitude, the peak frequency, and the parameters of the nonlinear system:

$$\mu = \frac{f\left|Y_1(0)\right|}{\omega p a}, \quad \varepsilon K_N = -\frac{8\omega q(\Omega-\omega)}{3p^2a^2}, \tag{27}$$

where $\omega = 86.44$ Hz is first natural frequency of the linear system, a is the peak amplitude of the nonlinear response function and $\Omega = 86.34$ Hz is the corresponding peak frequency. The parameters of nonlinear model, namely C andK_3, are calculated using Eq. (27) and are tabulated in Table 2.

A good agreement between the predictions of the identified nonlinear model and the measured responses are achieved as shown in Fig. 6.

Table 2
The identified joint parameters

K_1 (N/m)	K_θ (N/rad)	K_3 (N/m^3)	C (N s/m)
8.089×10^8	3264	3.722×10^8	0.281

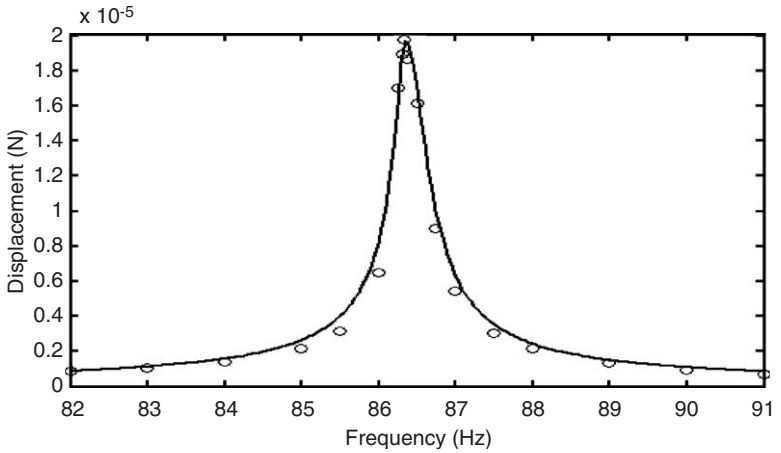

Fig. 6. The measured (circle) and predicted (solid line) frequency responses.

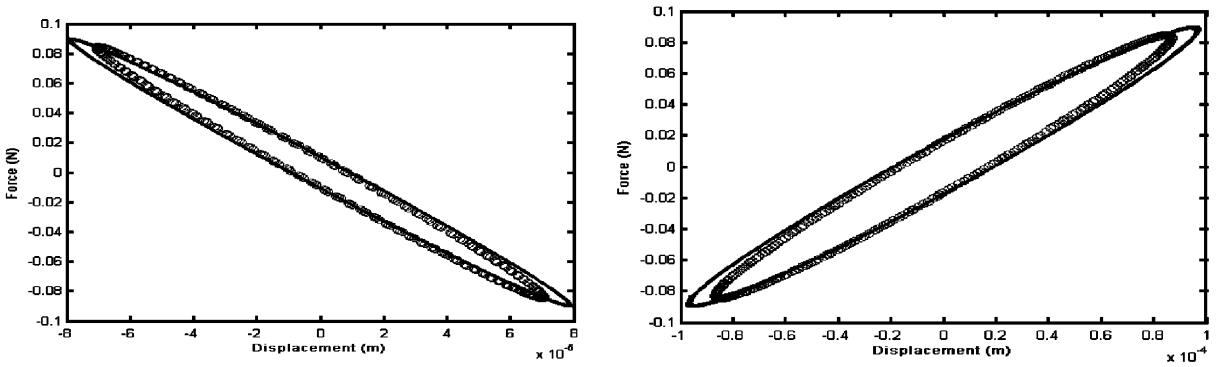

Fig. 7. The measured (circle) and predicted (solid line) hysteresis loops: left 86 Hz, right 86.75 Hz.

Fig. 7 shows the experimental and analytical hysteresis loops at 86 and 86.75 Hz. These two frequencies are just before and after the resonant frequency and loops clearly show a significant phase shift (close to 180°) due to the transition from resonant frequency. The experimental hysteresis loops are obtained by filtering the third-order super-harmony from the experimental responses.

6. Conclusions

A model for an Euler–Bernoulli beam with bolted lap joint in the mid span is presented. The joint is modelled using a nonlinear spring to represent the softening phenomenon of the joint interface due to slip. An approximate solution for the dynamical behaviour of assembled structure is obtained using the method of multiple scales. The solution provides frequency response function of the beam at any desired location due to a point excitation at a certain location. The obtained frequency response function is compared with the corresponding experimental counterparts to identify the parameters of the bolted joint interface. In the identification procedure joint interface parameters are fine tuned so that the differences between calculated and measured frequency responses are minimized.

References

[1] D.J. Segalman, T. Paez, D. Smallwood, A. Sumali, A. Arbina, Status and integrated road-map for joints modeling research, Sandia National Laboratories, SAND2003-0897, March 2003.
[2] E.F. Crawley, A.C. Aubert, Identification of nonlinear structural elements by force-state mapping, American Institute of Aeronautics and Astronautics Journal 24 (1986) 155–162.
[3] Y. Ren, T.M. Lim, M.K. Lim, Identification of properties of nonlinear joints using dynamic test data, American Society of Mechanical Engineers, Journal of Vibration and Acoustics 120 (1998) 324–330.
[4] Y. Ren, C.F. Beards, Identification of effective linear joints using coupling and joint identification techniques, American Society of Mechanical Engineers, Journal of Vibration and Acoustics 120 (1998) 331–338.
[5] X. Ma, L. Bergman, A.F. Vakakis, Identification of bolted joints through laser vibrometry, Journal Sound and Vibration 246 (3) (2001) 441–460.
[6] A. Ferri, Friction damping and isolation systems, American Society of Mechanical Engineers, Journal of Vibration and Acoustics 117 (1995) 196–206.
[7] L. Gaul, R. Nitsche, The role of friction in mechanical joints, Applied Mechanics Review 54 (2001) 93–106.
[8] R.A. Ibrahim, C.L. Pettit, Uncertainties and dynamic problems of bolted joints and other fasteners, Journal of Sound and Vibration 279 (3–5) (2005) 857–936.
[9] W.D. Iwan, A distributed-element model for hysteresis and its steady-state dynamic response, ASME Journal of Applied Mechanics 33 (1966) 893–900.
[10] Y. Song, C.J. Hartwigsen, D.M. McFarland, A.F. Vakakis, L.A. Bergman, Simulation of dynamics of beam structures with bolted joints using adjusted Iwan beam elements, Journal of Sound and Vibration 273 (1–2) (2004) 249–276.
[11] L. Gaul, J. Lenz, Nonlinear dynamics of structures assembled by bolted joints'', Acta Mechanica 125 (1997) 169–181.
[12] C.J. Hartwigsen, Y. Song, D.M. McFarland, L.A. Bergman, A.F. Vakakis, Experimental study of non-linear effects in a typical shear lap joint configuration, Journal of Sound and Vibration 277 (1-2) (2004) 327–351.
[13] H. Ouyang, M.J. Oldfield, J.E. Mottershead, Experimental and theoretical studies of a bolted joint excited by a torsional dynamic load, Materials Science Forum 440–441 (2003) 421–428.
[14] A.H. Nayfeh, D.T. Mook, Nonlinear Oscillations, Wiley Interscience, New York, 1979.
[15] M. Pakdemirli, H. Boyacy, Non-linear vibrations of a simple–simple beam with a non-ideal support in between, Journal of Sound and Vibration 268 (2) (2003) 331–341.
[16] P. Malatkar, Nonlinear vibration of cantilever beams and plates, Ph.D. Thesis, Virginia Polytechnic Institute and State University, Blacksburg, Virginia, July 2003.